Noninvasive Probing of the Ocean Surface Using Laser-Based Nonlinear Optical Methods*

Abstract

The laser based nonlinear optical methods of second-harmonic generation and sum-frequency generation have been developed to study the chemical composition and concentration of natural surfactant materials present as slicks on the ocean surface. These noninvasive second-harmonic and sum-frequency generation methods produce signals which originate from only the top few molecular layers of the ocean surface, thereby producing an accurate picture of the ocean surface condition without interference from the bulk ocean chemistry. Chemical specificity of the methods is achieved by tuning the incident laser frequency to coincide with optical absorptions in the surface absorbed materials.

Introduction

The sea/air interface covers greater than 70 percent of the Earth's surface. There are a number of interrelated physical and chemical phenomena associated with this interface that make it of great environmental importance. The physical properties of the sea/air interface are strongly controlled by the chemical character of the ocean surface layer. The thin surface region of the ocean, about 1 mm thick, is often referred to as the sea-surface microlayer and it is known to control the properties of the sea/air interface. The microlayer surface region has a diverse chemical composition resulting from biogenic production of surface-active compounds (Williams *et al.*, 1986; Hardy, 1991). In addition to concentrating naturally occurring organic compounds, the interface is also a sink for anthropogenic trace metals and other organic pollutants (Hardy, 1987). The composite chemical character of the surface microlayer plays an important role in wind-wave coupling (Scott, 1972), air/sea gas exchange (Brockmann *et al.*, 1982), and the reflection and transmission of electromagnetic radiation from the ocean interface (Hühnerfuss *et al.*, 1986; Scully-Power, 1984).

There is a growing interest in and need to understand the chemical, physical, and biological nature of the sea-surface microlayer. Traditional methods used to study the microlayer involve invasive sampling where the ocean surface is skimmed to remove the surface layer for chemical analysis (Hardy *et al.*, 1988; Carlson *et al.*, 1988; Frew and Nelson, 1992a; Frew and Nelson, 1992b). Unfortunately, these methods disrupt the natural structure of the microlayer and sample a water layer about 60 μm deep. It may be argued, however, that the physical properties of the ocean surface are controlled by a surface layer confined to several molecular layers or about 1 nm. This is because surface tension, surface elasticity, and surface visocity are most affected by the chemical composition of the top few molecular layers (Adamson, 1982).

Noninvasive, *in situ* methods for studying the microlayer are needed because the molecular surface of the air/sea interface must be studied undisturbed and in its natural state. Over the last five years we have been experimenting with laser-based second-order nonlinear optical processes as *in situ* ocean surface probes. The nonlinear processes of reflected second-harmonic generation (SHG) and reflected sum-frequency generation (SFG) have emerged as powerful interfacial spectroscopic probes for laboratory studies (Shen, 1989). These probes are capable of determining the molecular composition, concentration, and molecular level structure of a surface layer. We have successfully extended these spectroscopic methods for use as an *in situ* remote sensing probe of the surface microlayer. The research presented here represents the first instance of *in situ* ocean surface spectroscopy. The success of the SHG and SFG experiments leads directly to future applications using more versatile and powerful nonlinear optical probes. This paper contains a summary of current research results and future directions for nonlinear optical study of the ocean interface.

Background

The theoretical background of nonlinear optics and laboratory experimental procedures for reflected SHG and SFG interfacial spectroscopy has been reviewed in detail elsewhere (Shen, 1984; Shen, 1989; Richmond *et al.*, 1988) with detailed discussions of SHG and SFG applied to ocean studies included in earlier papers (Frysinger *et al.*, 1992; Korenowski *et al.*, 1989; Asher *et al.*, 1988). Although detailed presentation of this background material is beyond the scope of this paper, the following summary should provide the reader a basic understanding of nonlinear optical theory and techniques.

The nonlinear optical signal observed from an ocean surface results from an interfacial macroscopic polarization induced by an impinging high intensity light beam. The macroscopic polarization is expressed as a power series expansion in the electric fields of the incident light with proportionality constants that are the corresponding optical susceptibilities of the interface. These susceptibilities are a

*Presented at the First Thematic Conference on Remote Sensing for Marine and Coastal Environments, New Orleans, Louisana, 15-17 June 1992.

Gerald M. Korenowski, Glenn S. Frysinger, and **William E. Asher†**
Department of Chemistry, Rensselaer Polytechnic Institute, Troy, NY 12180-3590.

†Presently with Battelle Marine Sciences Laboratory, Sequim, WA.

Photogrammetric Engineering & Remote Sensing, Vol. 59, No. 3, March 1993, pp. 363–369.

0099-1112/93/5903–363$03.00/0

©1993 American Society for Photogrammetry and Remote Sensing

function of the surface material's internal vibrational and electronic structure. It is the second term in the power series, defined as the second-order nonlinear optical polarizability, and given explicitly by

$$\vec{P}^{(2)}(\omega_3 = \omega_1 + \omega_2) = \overleftrightarrow{\chi}^{(2)} : \vec{E}(\omega_1)\vec{E}(\omega_2) \quad (1)$$

that gives rise to second-harmonic and sum-frequency processes. In the dipole approximation, the second-order term is forbidden in bulk ocean water because the structure is isotropic and possesses inversion symmetry on the dimensional scale of the light beams. At the air/water interface, however, the isotropy is broken, giving rise to a nonlinear optical reflection at the optical frequency of the induced nonlinear polarization ω_3. If a single incident laser frequency is used, the nonlinear optical reflection is called the second-harmonic and is twice the incident laser frequency. If two different frequency lasers are used, the resulting nonlinear signal is at the sum of the laser frequencies. If the medium containing the reflection is nondispersive, or weakly dispersive like air, the reflected incident laser beam and reflected SHG signal are collinear.

The collinearity of the linear and nonlinear reflection provides a method for scaling the nonlinear optical signal because the laser reflection and collinear nonlinear signal will have equal collection probability. Therefore, signal loss is equal for both the laser reflection and nonlinear signal. In the case of *in situ* measurements, loss occurs because the wave structure on the ocean surface produces divergent and angularly scattered reflections. Because the incident laser intensity is known, the ocean reflection may be calculated from Fresnel formulae (~ 2 percent laser reflection for a nadir geometry). The detector-system-measured laser reflection may then be used to scale the nonlinear signal to remove surface scattering uncertainties.

The intensity of the reflected nonlinear optical signal produced at the ocean interface is a function of the chemical composition of the interface and is reflected in the second-order nonlinear optical susceptibility of the interface. To a first approximation, the susceptibility is expressed as the surface density of the molecular species multiplied by the nonlinear optical molecular polarizability of the molecule, and, for multi-component systems, the total susceptibility is the sum of the individual component's susceptibilities. The nonlinear molecular polarizability is related to the linear polarizability, and, in similarity with the linear polarizability, the nonlinear polarizability exhibits vibrational and electronic resonances. The resonances dramatically increase the nonlinear optical reflection intensity when the incident laser beam or nonlinear signal frequency is equal to a vibrational or electronic optical transition frequencies. Therefore, with a frequency-tunable laser source, the nonlinear optical process can be used for spectroscopic analysis of the ocean surface layer.

Other second-order nonlinear optical processes include difference-frequency generation ($\omega_3 = \omega_1 - \omega_2$) and optical rectification ($0 = \omega_1 - \omega_1$). Optical rectification may be a particularly promising interfacial probe for the ocean and will be discussed in more detail later.

Experimental

The data presented in this paper were obtained from three different field experiments. The first was conducted from a pier at the Woods Hole Oceanographic Institution (WHOI) during June 1988; the second was conducted from the Chesapeake Light Tower off of Cape Henry, Virginia, during SAXON-88, October 1988; and the third was conducted in the Pacific Ocean from the the R/V *Wecoma* near Santa Cruz and Santa Rose during SLIX-89, October 1989.

The experimental apparatus used in each of the field experiments were identical except for minor modifications. The laser source was a Q-switched Nd:YAG laser producing 20-Hz, 9×10^{-9} sec pulses at 1064 nm, 532 nm, and 355 nm. The SHG experiments used a 532-nm, 0.35-J, laser beam to produce a nonlinear optical signal at 266 nm. The SFG experiments used both the 532-nm, 0.35-J, and 355-nm, 0.15-J, laser beams to generate a nonlinear optical signal at 213 nm. In either optical configuration, the unfocused, 2.5-cm-diameter laser beams were directed to the ocean surface with prisms using a nadir incident laser beam and signal collection geometry (Figure 1). A Newtonian telescope with a 0.4-m-diameter primary mirror was used to collect both the laser reflection and reflected nonlinear optical signal. In the WHOI pier experiment, the telescope was located at the end of a pier with a primary mirror positioned 4.5 m above the ocean surface. In the SAXON-88 tower experiment, the telescope and turning prism were mounted 9.5 m outboard and 5 m above the ocean surface. In the SLIX-89 experiment, the telescope and turning prism were located approximately 4 m outboard the port side of the ship and 6 m above the ocean surface.

The telescope detector system includes an optical detector box attached to the side of the telescope. This detector box contains colored glass filters, interference filters, and photomultiplier tube detectors to measure the intensity of both the linear laser reflection and the nonlinear SHG or SFG signal. The PMT signals are preamplified at the telescope and transmitted via coaxial cables to a gated integrator for discrimination of the pulsed signals and subsequent computer digitization and storage. Additional details of the experimental apparatus and procedures can be found in Frysinger *et al.* (1992) and Korenowski *et al.* (1989).

Results and Discussion

Verification that the UV light measured by the PMT was an SHG or SFG signal was achieved by measuring the signal's temporal pulse width, wavelength, wavelength bandwith, and laser intensity dependence of the signal. The most straightforward check for verifying that the detected signal results from a second-order nonlinear optical process is to show that the signal intensity varies as the square or product of the incident laser beam intensities for SHG and SFG processes, respectively. Comparison of these results with predictions based on nonlinear optical theory proved that the observed UV signals were SHG or SFG signals in each experiment.

Additional studies have shown that the detected nonlinear optical signal was generated only at the ocean surface

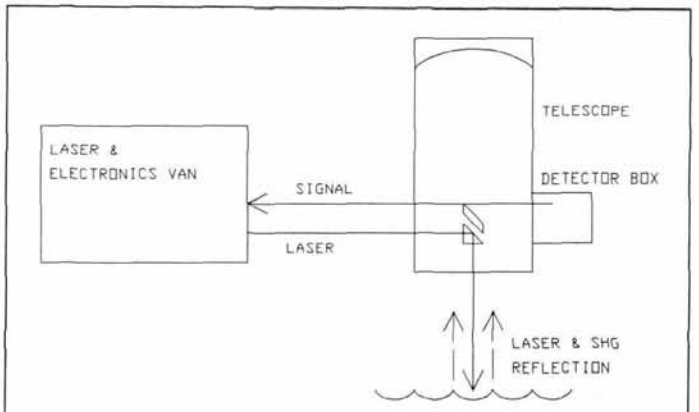

Figure 1. SHG and SFG Experimental Schematic.

(Frysinger *et al.*, 1992). It was also determined that the detected laser reflection is dominated by the surface reflection; the bulk water backscattering is much less intense. Confirming that both signals originate at the ocean surface allows accurate scaling of the nonlinear signal with the intensity of the laser reflection.

Typically, the SHG or SFG signal, laser reflection intensity, wind speed, and other measurements were measured and digitized at the 20-Hz repetition rate of the laser to form a time series. Figure 2 is an example time series recorded during the pier experiment conducted at WHOI on 10 June 1988. The SHG signal at 266 nm is seen in Figure 2a, the 532 nm laser reflection is seen in Figure 2b, and the accompanying wind speed record is seen in Figure 2c. The data in these time series have been averaged over a two-second interval to remove shot-to-shot variations. The remaining signal structure is due to changes in chemical composition at the ocean surface, surface gravity waves, and surface roughness due to wind stress. Because no visible surface slicks were present during this period, the naturally occuring surface-active organic concentration on the ocean surface was too small to produce wave damping. However, concurrent *ex situ* measurements performed by surface skimming and film trough analysis indicated the presence of small quantities of surfactant in the skimmed surface samples (top 60 μm). Therefore, the data in Figure 2 represent the SHG signal laser reflection intensity of a typical patch of ocean surface.

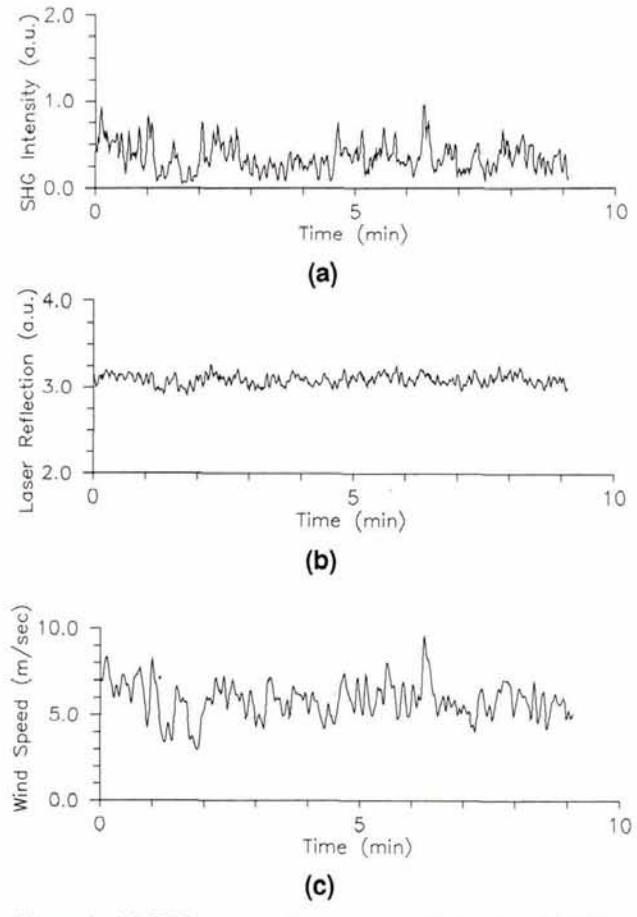

Figure 2. (a) 266-nm SHG time series, 10 Jun 88. (b) 532-nm laser reflection time series, 10 Jun 88. (c) Wind speed SHG time series, 10 Jun 88.

In order to help understand how the nonlinear optical and linear reflections are affected by wind speed and the resulting ocean surface roughness, cross-correlations between wind speed and SHG intensity, wind speed and laser reflection intensity, and laser reflection and SHG intensities were calculated. The 12,000-point (12,000 laser shot) data set from Figure 2a-2c shows typical data used for this analysis and was chosen because cross-correlation estimates require a stationary time series (Bendat and Piersol, 1971). The 12,000-point data set was divided into nine separate records, each containing 1250 data points or 62.5 sec of data. Before the cross-correlation was estimated, each 1250-point sub-set was running-mean filtered with a two-second window to remove shot-to-shot noise. The discrete, circular cross-correlation estimate is defined by Bendat and Pierson (1971) as

$$R_{XY}(i) = (1/N) \sum_{j=1}^{N} X(j)Y(j + 1)/(s_X s_Y)^{1/2} \qquad (2)$$

where X and Y denote the two time series (i.e., wind, 532-nm laser signal, or 266-nm SHG signal), N is the total number of data points per set, and s_x and s_y are the variances of X and Y, respectively. $R_{xy}(i)$ was calculated using a circular convolution Fast Fourier Transform algorithm and the nine sub-sets were point-by-point averaged to reduce the overall variance in estimating $R_{xy}(i)$. The averaged estimate of $R_{xy}(i)$ is shown in Figure 3a for wind (U) and 266-nm SHG signal, Figure 3b for U and 532-nm signal, and Figure 3c for 532-nm and 266-nm signals. The comparison of the $Rxy(0)$ magnitude with standard tables shows each is statistically significant at the 1 percent level. This implies that the three pairs of data are correlated (Jenkins and Watts, 1969).

The correlation of wind speed with the SHG and reflected laser signals is expected because the ocean surface becomes rougher on the scale of the laser footprint due to capillary wave generation as the wind speed increases or gusts. Although still directional, the scattering from a wave-roughened surface is more diffuse and Lambertian in character, leading to a greater possibility that, for any given laser pulse, a portion of the linear or nonlinear optical reflection is captured by the telescope system. This leads to an overall increase in the average signal detected. Both the SHG and laser reflection signal show a time lag in their maximum cross-correlation with wind speed. The time lag in these cross-correlations is also expected because the anemometer recording the wind speed was positioned 5 m above the ocean surface and a delay is expected between surface wave structure formation and small recorded wind gusts.

The maximum value of the cross-correlation between the wind speed and the 532-nm laser reflection shown in Figure 3b is substantially less than that between the wind speed and the 266-nm SHG signal shown in Figure 3a. This indicates that the increases in wind speed and surface roughness increase the nonlinear optical signal more than the reflected laser intensity. This larger effect of wind on SHG signal may be caused by a fundamental difference in the depths at which generation of the nonlinear optical signal and reflection of the incident laser beam occurs.

As discussed earlier, the SHG signal is generated in a water surface layer approximately 1-nm deep. In constrast, linear reflection occurs in a surface layer defined by the incident laser wavelength, in this case about 500 nm (Shen, 1984). Therefore, because changes in surface chemical composition occur mostly in the 1-nm layer, they will have a large effect on the SHG signal but little effect on the reflected laser intensity. Although the roughening of the water surface affects both the SHG and reflected laser intensities through

Lambertian scattering as described above, the wind stress also affects the surface chemical composition through the surface dilatation and turbulence of capillary waves. These chemical changes will affect the SHG signal but not the reflected laser intensity, leading to a larger maximum cross-correlation value between wind-speed and 266-nm intensity than between wind speed and 532-nm laser reflection intensity. Furthermore, because the maximum cross-correlation value increases, increases in wind speed must increase the SHG signal more than increases in the wind speed increase the reflected laser intensity.

The explanation presented above is supported by the cross-correlation between the reflected 532-nm laser intensity and the 266-nm SHG signals. As expected, and shown in Figure 3c, there is zero time lag in the maximum cross-correlation value between the SHG signal and reflected laser intensity. This suggests that the laser pulse occurring when the SHG signal is measured is the most important laser pulse in determing the nonlinear optical response. However, given the nonlinear dependence of the SHG signal on the incident laser beam, the correlation is not as strong as expected if the only factor affecting the SHG and reflected signals is the physical Lambertian scattering mechanism discussed above. Therefore, because the cross-correlation of the reflected laser intensity and SHG intensity is lower than expected, it may be assumed that some factor other than incident laser power is also important in determing the observed SHG signal intensity. The data suggest that this second factor is most likely a

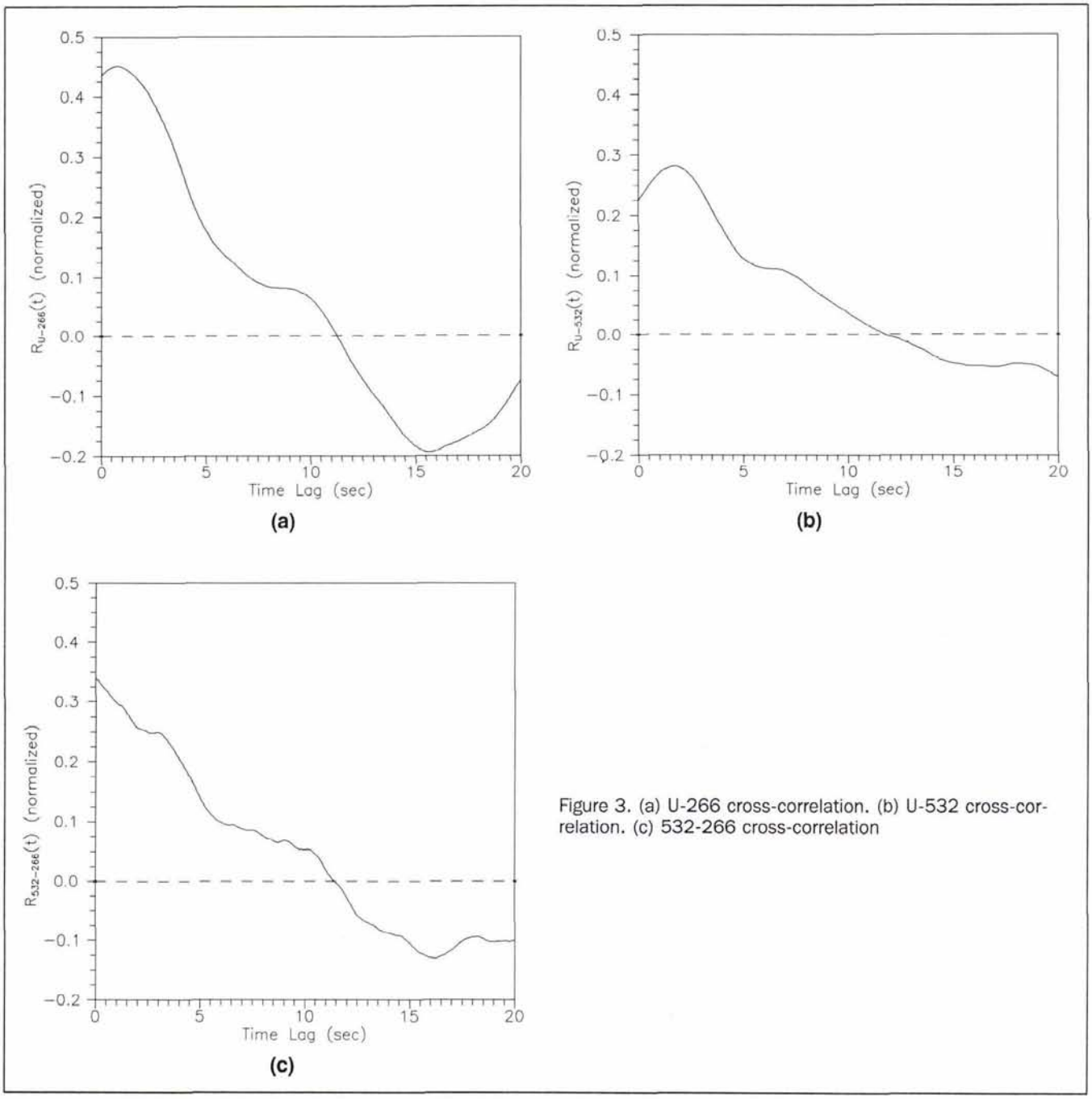

Figure 3. (a) U-266 cross-correlation. (b) U-532 cross-correlation. (c) 532-266 cross-correlation

change in surface chemical composition caused by wind-roughening of the surface.

Because it is generally assumed that wave action and wind stress reduce the concentration of surface-active compounds at the surface through capillary waves and turbulence, these cross-correlation results imply that naturally occurring surfactants decrease the observed 266-nm SHG signal. Therefore, natural surfactants must have small nonlinear susceptibilities at the wavelengths used in these experiments with respect to the nonlinear susceptibility of the surfactant-free ocean surface. In fact, lipid materials, known to be present in the ocean surface (Williams *et al.*, 1976; Frew and Nelson, 1992a; Frew and Nelson, 1992b), have smaller nonlinear susceptibilities compared to the uncontaminated ocean surface and compared to more soluble naturally occurring surface-active material. This, and the data presented below, suggest that the interpretation of the cross-correlation results described above is correct.

The nonlinear susceptibility of the slicked and nonslicked ocean surface was studied during the SAXON-88 tower experiment. Figure 4 contains 266-nm SHG signals measured during the SAXON-88 tower experiment on 1 October 1988. Environmental conditions include a 2.0 to 3.0 m sec^{-1} wind speed from 75° and a 0.7 m significant wave height (SWH). The SHG time series has three periods of SHG signal decrease labeled A, B, and C. These decreases occur even though the wind speed and incident laser intensity remained constant throughout the time period. These periods of SHG signal decrease were caused by the passage of natural ocean slicks through the laser-sampling area. The slicks were identified visually as ocean regions exhibiting damped surface ripple structure and quantitatively by reduced surface tension measurements made by calibrated spreading oils (Adam, 1937) and *ex situ* sampling (Frysinger *et al.*, 1992; Barger, 1986). Therefore, the data shown in Figure 4 demonstrate that visible surface slicks composed of naturally occuring surfactants drastically reduce the SHG signal intensity.

In order to provide a known ocean surface chemical composition for testing the nonlinear optical response between slicked and nonslicked regions, man-made slicks of polyethylene glycol 200 monolaurate (PEG-ML) were generated and allowed to drift through the laser-sampling area during the SAXON-88 experiment. Because PEG-ML spreads to form a uniform monolayer and because its interfacial behavior has been found to resemble naturally occurring surfactants (Barger and Means, 1985), it provides a known interfacial chemical composition to test the effect on SHG intensities. Furthermore, because PEG-ML is essentially a saturated hydrocarbon, its nonlinear optical susceptibility will be low compared to a nonslicked ocean surface.

Figure 5 shows the reflected SHG signal intensity measured from a PEG-ML slicked ocean surface during SAXON-88 on 9 October 1988. The passage of four PEG-ML slicks indicated by regions labeled A, B, C, and D produces a decrease in the SHG intensity. During the measurement period, the wind speed was 3.0 m sec^{-1} from 115° with a 2.0-m SWH. The SHG signal decrease indicates that the presence of PEG-ML on the ocean surface decreased the SHG signal relative to the nonslicked water surface. In similarity with the effects of naturally occurring surface slicks, the decreases seen in Figure 5 are most likely due to a decrease in the SHG response of the slicked surface.

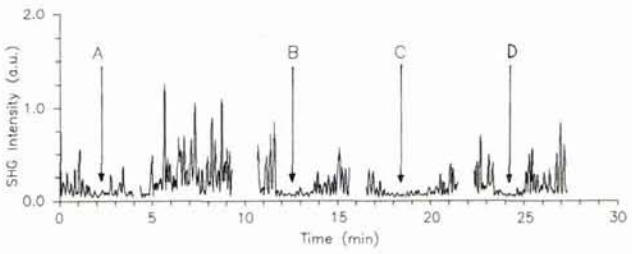

Figure 5. SHG time series from artifical slicks, 09 Oct 88.

In agreement with theory, the data from the WHOI pier experiment and from SAXON-88 indicate that second-order nonlinear processes are highly surface selective. In addition, these nonlinear processes are very sensitive to changes in chemical composition of the top few molecular layers of the ocean surface. Finally, the observed SHG signal at 266 nm from the ocean surface was observed to be larger for the nonslicked regions than for areas covered by either naturally occurring slicks or by artificial slicks composed of PEG-ML. This implies that these surface-active materials lower the effective second-order nonlinear susceptibility of the sea surface at the wavelengths studies.

In the SLIX-89 ship-based experiment, two new aspects were added to the experiment. First, the probe system was mounted aboard a ship to increase sampling mobility, and second, a different wavelength combination for the nonlinear optical reflection was employed. For 266-nm SGH generation using a 532-nm probe, lipids and other strongly surface-active materials proved less nonlinear than the ocean substrate. Alternative incident laser wavelengths which produce an increasing nonlinear optical signal with increasing surfactant concentration would be a more useful probe of microlayer organics. Exploiting the fact that lipid surfactants have electronic resonances in the 210-nm far UV wavelength region, the combination of 532-nm and 355-nm laser beams was chosen to produce a 213-nm surface SFG reflection. At 213 nm, a substantial resonance enhancement of the surfactant produced signal is expected.

Figure 6 shows a time series of SFG signal measured dur-

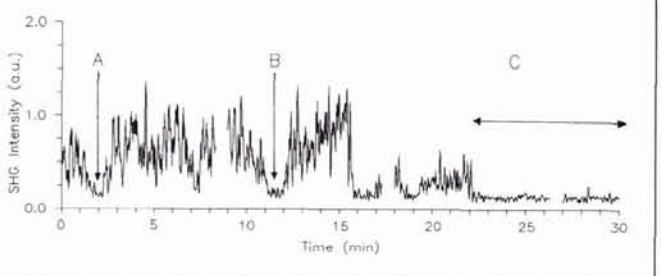

Figure 4. SHG time series from natural slicks, 01 Oct 88.

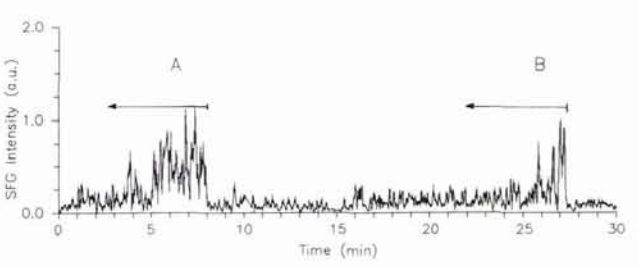

Figure 6. SFG Time series from natural slicks, 18 Oct 89.

ing the SLIX-89 ship experiment on 18 October 1989. Environmental conditions include a 5.0 m sec^{-1} wind speed from 300° and a ship heading of 270° at 1.0 m sec^{-1}. The regions of increased SFG signal labeled A and B correspond to the presence of natural banded slicks in the laser-sampling area. The ship and laser probe transected these banded ocean slicks from the down-wind to up-wind direction with the largest SFG signals observed at the up-wind edge of the slicks. It is assumed that the increasing 213-nm SFG signals correspond to increasing natural surfactant concentrations.

It is particularly interesting that the surfactant concentration as measured by the SFG probe was not uniform across the banded slicks studied during the SLIX-89 experiment. This raises questions about the factors creating and maintaining the surfactant concentration gradient. Bulk hydrodynamic forces, interfacial chemical forces, and wind are all potential factors in shaping the surfactant concentration in banded slicks. In this particular experiment, although hydrodynamic forces are unknown, wind forces can adequately explain the concentration gradient. Wind drag on the up-wind edge of the slick will inhibit natural surface film expansion, while contributing to natural surfactant spreading on the down-wind edge of the slick. As a result, the up-wind edge of the slick will exhibit higher organic concentrations and greater film pressures (Barger *et al.*, 1970; Barger, 1974; Barger, 1991). The type of surface concentration data obtained with this 213-nm SFG probe shows promise in providing information necessary for understanding slick formation and maintenance and other ocean interfacial phenomena.

A structural model of the natural surfactant film can be inferred from the 213-nm SFG data of Figure 6. The SFG probe can differentiate between monolayer or "monolayer-type" and multilayer surface slicks. In a multilayer slick, the surface concentration in the top molecular layer does not vary across the surface film and the SFG signal should exhibit a step function response at the slick edges. This is not like the situation depicted by Figure 6 where a variable SFG signal and variable surface concentration exists. The natural banded slicks observed during SLIX-89 have SFG signals indicating monolayer-type, not multilayer structure. This analysis of SFG signal gradient has the potential to be used for distinguishing monolayer-type films of natural surfactants from mutiliayer surface film such as petroleum slicks. However, the most powerful chemical information derived from SHG and SFG probes will come from exploiting their spectroscopic capabilities.

SHG and SFG experiments performed with tunable incident laser sources will allow *in situ* ocean surface spectroscopy. This capability has already been accomplished in laboratory studies, but the intensity and tunability of laser sources has made field experiments more difficult. One possible field study application would include a tunable near-infrared laser operating over the spectral region 2.5 to 1.0 μm. This wavelength region falls between the standard mid-infrared region of vibrational spectroscopy and the visible wavelength region of electronic absorption spectroscopy. Although not often used in spectroscopic studies, it is in this wavelength region where the vibrational overtone absorptions of organics are found. The near-infrared spectral region is also less cluttered than the mid-infrared spectral region because only the overtones of strong vibrational absorptions can be seen. This would lead to easier identification of classes of organics found in the complex mixtures which exist at the sea/air interface. The vibrational or near-infrared spectra are also more useful in identifying the chemical character of the species than is UV-visible electronic absorption spectroscopy. However, problems would exist with such a near-infrared SHG or SFG experiment such as the detection of the signal against a strong solar background and that the detection system efficiency changes as the nonlinear optical signal wavelength varies. Even more promising because these problems are absent is the nonlinear optical process of optical rectification.

Optical rectification is related to SHG and SFG in its origin and would possess many of the same characteristics, including its molecular scale surface selectivity. In SHG, the optical frequencies are summed to produce a macroscopic material polarization and reradiation at the sum frequency, $\omega_2 = \omega_1 + \omega_2$. In comparison, the rectification process produces a material polarization at a zero frequency, $0 = \omega_1 - \omega_1$. It may be expected that a zero frequency polarization will not radiate electromagnetic radiation. However, when a pulsed laser system is the driving source, the surface polarization appears and disappears over the temporal duration of the driving laser pulse and this oscillating on/off DC polarization will electromagnetically radiate. A Fourier analysis of the temporal character of the laser pulse yields the spectral frequencies emitted by the interfacial optical rectification polarization. Interestingly, the emitted spectral frequencies are dependent only on the laser pulse shape and duration and not on the wavelength of the incident laser radiation. Laser pulses ranging from several picoseconds to tens of picoseconds would result in optical rectification emissions at frequencies from several gigahertz to several hundred gigahertz. Consequently, the frequency region of the surface microwave return could be selected by choosing a laser pulse width to produce radiation where there is a corresponding high atmospheric transmission window. A simple schematic of such an experimental arrangement is given in Figure 7. In this experimental configuration, a radiometer would be substituted for the optical telescope.

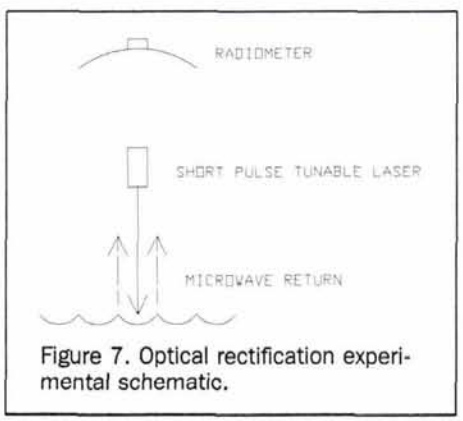

Figure 7. Optical rectification experimental schematic.

Conclusions

In conclusion, we have shown that laser-based second-order nonlinear optical processes of SHG and SFG provide highly surface selective, noninvasive, *in situ* probes of the ocean surface. Although preliminary experiments were reported in this paper, the probes provide important information about the nature of surfactants at the ocean surface and their behavior in response to dynamic forces at the sea/air interface. The future of the probes lies in their further development and use as *in situ* interfacial spectroscopic techniques.

Acknowledgments

The authors wish to thank the many scientists involved in the success of the field experiments. N.M. Frew and R. K. Nelson hosted the pier experiment at WHOI. O. H. Shemdin served as chief scientist and experimental coordinator for the

SAXON-88 tower experiment. D. J. Carlson served as chief scientists for the SLIX-89 ship experiment. Many helpful discussions with F. Herr of the Office of Naval Research are acknowledged. This research was supported by the Office of Naval Research under contract N0001487LK0239 and grant N0001490J1537. W. E. Asher acknowledges partial support by the U.S. Department of Energy under contract DE-AC06-76RLO-1830.

References

Adam, N. K., 1937. A rapid method for determining the lowering of tension of exposed water surfaces, with some observations on the surface tension of the sea and of inland waters, *Proc. R. Soc. London, Ser. B*, 122:134-139.

Adamson, A. W., 1982. *Physical Chemistry of Surfaces*, 4th ed., John Wiley, New York, N.Y.

Asher, W. E., G. S. Frysinger, and G. M. Korenowski, 1988. Reflected optical second-harmonic generation in the study of naturally occurring organic films at the ocean surface, *J. Geophys. Rec.*, 93C:6955-6957.

Barger, W. R., 1974. Surface chemical properties of banded sea slicks, *Deep-Sea Res.*, 21:83-89.

———, 1986. *Naturally-Occurring Surface Active Material Concentrated at the Air/Water Interface*, Ph.D. thesis, University of Maryland, College Park.

———, 1991. *A Review of Experimental Observations and Remaining Questions Concerning Formation, Persistence, and Disappearance of Sea Slicks*, NRL report 9313, Naval Research Laboratory, Washington, D.C., May 6, 1991.

Barger, W. R., W. D. Garrett, E L. Mollo-Christensen, and K. W. Ruggles, 1970. Effects of an artficial sea slick upon the atmosphere and the ocean, *J. Appl. Meteorol.*, 9:396-400.

Barger, W. R., and J. C. Means, 1985. Clues to the structure of marine organic material from the study of physical properties of surface films, *Marine and Estuarine Geochemistry* (A. C. Sigleo and A. Hattori, editors), Lewis, Chelsea, Michigan, pp. 47-67.

Bendat, J. S., and A. G. Piersol 1971. *Random Data; Analysis and Measurement Procedures*, John Wiley, New York.

Brockmann, U. H., H. Hühnerfuss, G. Kattner, H.-C Broecker, and G. Hentzschel, 1982. Artificial surface films in the sea area near Sylt, *Limnol. Oceanogr.*, 27:1050-1058.

Carlson, D. J., L. L. Cantey, and J. J. Cullen, 1988. Description of and results from a new surface microlayer sampling device, *Deep Sea Res.*, Part A, 35:1205-1213.

Frew, N. M., and R. K. Nelson, 1992a. Isolation of marine microlayer film surfactants for ex situ study of their surface physical and chemical properties, *J. Geophys. Res.* 97C:5281-5290.

———, 1992b. Scaling of marine microlayer film pressure-area isotherms using chemical attributes, *J. Geophys. Res.* 97C:5291-5300.

Frysinger, G. S., W. E. Asher, G. M. Korenowski, W. R. Barger, M. A. Klustry, N. M. Frew, and R. K. Nelson, 1992. Study of ocean slicks by nonlinear laser processes. 1. Second-harmonic generation, *J. Geophys. Res.* 97C:5253-5269.

Hardy, J. T., 1987. Anthropogenic alteration of the sea surface, *Mar. Environ. Res.*, 23:223-225.

———, 1991. Where the sea meets the sky, *Natural History*, May 1991, pp. 59-65.

Hardy, J. T., J. A. Coley, L. D. Antrim, and S. L. Kiesser, 1988. A hydrophobic large-volume sampler for collecting aquatic surface microlayers: Characterization and comparison with the glass plate method, *Can J. Fish Aquat Sci.*, 45:822-826.

Hühnerfuss H., W. D. Garrett, and F. E. Hoge, 1986. The discrimination between crude-oil spills and monomolecular sea slicks by an airborne lidar, *Int. J. Remote Sensing*, 7:137-150

Jenkins, G. M. and D. G. Watts, 1968. *Spectral Analysis and its Applications*, Holden Day, Oakland, Calif.

Korenowski, G. M., G. S. Frysinger, W. E. Asher, W. R. Barger, and M. A. Klusty, 1989. Laser based nonlinear optical measurement of organic surfactant concentration variations at the air/sea interface, *Proceedings International Geoscience and Remote Sensing Symposium*, IEEE 89CH2768-0 Inst of Elect. and Electron Eng, New York, vol. 3, pp. 1506-1509.

Richmond, G. L., J. M. Robinson, and V. L. Shannon, 1988. Second harmonic generation studies of interfacial structure and dynamics, *Prog. Sur. Sci.* 28:1-70

Scott, J. C., 1972. The influence of surface-active contamination on the initiation of wind waves, *J. Fluid Mech.*, 56:591-606.

Scully-Power, P. J., 1984. *Aviation Week and Space Technology*, October 29, pp. 54-55.

Shen, Y. R., 1984. *The Principles of Nonlinear Optics*, chap. 1 and 25, pp. 1-12, 479-504, John Wiley, New York.

———, 1989. Surface properties probed by second-harmonic and sum-frequency generation, *Nature*, 337:519-525.

Williams, P. M., A. F. Carlucci, S. M. Henrichs, E. S. Van Vleet, S. G. Horrigan, F. M. H. Reid, and K. J. Robertson, 1986. Chemical and microbiological studies in the Southern Gulf of California and off the West coast of Baja California, *Mar. Chem.* 19:17-98.

LIST OF "LOST" CERTIFIED PHOTOGRAMMETRISTS

We no longer have valid addresses for the following Certified Photogrammetrists. If you know the whereabouts of any of the persons on this list, please contact ASPRS headquarters so we can update their records and keep them informed of all the changes in the Certification Program. Thank you.

Dewayne Blackburn	George Glaser	Spero Kapelas	James Steckling
Albert Brown	William Grehn, Jr.	Francisco Milande	Keith Syrett
Eugene Caudell	Elwood Haynes	Harry J. Miller	William Thomasset
Robert Denny	F.A. Hildebrand, Jr.	Marinus Moojen	Conrad Toledo
Leo Ferran	James Hogan	Gene A. Pearl	Robert Tracy
Robert Fuoco	William Janssen	Sherman Rosen	Lawrence Watson
Franek Gajdeczka	Lawrence Johnson	Lane Schultz	Tad Wojenka